

Kpkkcn'Xqnci g'Cpi ng'F gwgekqp'O gyj qf "qh'c'RY O" Eqpxgtvgt'y kj qw'cp{ 'I tkf 'Xqnci g'O gcuwtgo gpv' Wukpi 'Eqpf wekqp'Ucvwg"qh'F kqf gu'hqt'Uo qqj 'Uctvki

Jae-Jung Jung, Eunsoo Jung, Jung-Ik Ha, and Seung-Ki Sul

Department of Electrical and Computer Engineering,

Seoul National University

1 Gwanak-ro, Gwanak-gu, Seoul 151-744, Republic of Korea

jjjzzz@eepel.snu.ac.kr

Abstract—Accurate detection of the grid angle at the startup of a converter prevents the over-current trip and also reduces the commissioning time of the system. This paper presents a method to detect initial angle of the grid voltages by measuring the phase currents depending on conduction state of diodes. During the diode conduction, the source voltages are estimated and the estimated voltages are fed into phase locked loop (PLL). When all the diodes are turned off, the source voltage estimator and the PLL are bypassed and the voltage angle is calculated from the frequency of the estimated voltages. The feasibility of the proposed method has been verified by computer simulation and experimental results.

Keywords- *initial angle detection, pulse width modulation (PWM) converter, grid angle, voltage source sensorless converter*

I. INTRODUCTION

Three-phase Pulse Width Modulation (PWM) converters are utilized in many applications where dc-link voltage control, low harmonic input current or power factor control is required [1]-[4]. In the PWM converters, source voltage information is used for the field orientation in the convertor power control, a feed-forward term for current controller, and grid synchronization in the case of using Phase Locked Loop. In addition, the source voltage angle is used for a synchronous reference frame transformation in the current controller. Therefore, the source voltage information is essential to control PWM converter.

In many conventional systems, voltage sensors have been used to obtain source voltage information. But these voltage sensors increase the cost and also threaten the reliability of the system. Therefore, the control strategies for PWM converter without the source voltage sensors have been introduced in [5]-[9]. For the sensorless operation, the error of the estimated source voltage has to converge near zero for smooth starting. If the error is not small enough, it causes instability in control at the start-up of the PWM converter. Additionally, the uncontrolled current during the transient may cause dc-link over-voltage trip when the dc-link capacitance is too small to endure the uncontrollable energy and over-current also may

occur depending on the capacity of the interface inductance. Therefore, detecting initial angle at the startup contributes to the proper and safe operation of the PWM converter.

For the initial angle detection, the methods based on the change of the phase currents during zero voltage output are introduced in [10]-[12]. However, a large amount of phase currents are likely to flow because the zero voltage vector makes short status in the source circuit. The large currents cause additional loss and prevent reducing the size of the interface inductor. Furthermore, because this method uses change of the phase currents for very short time interval, the measurement error may give rise to obtain wrong initial angle.

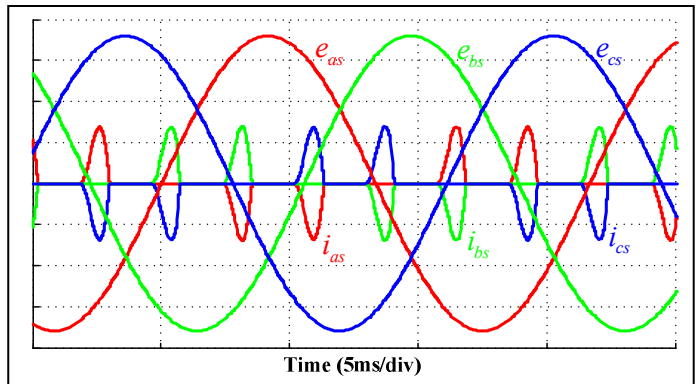


Figure 1. Simulation waveforms of line-to-neutral source voltages in 50V/div(e_{as} , e_{bs} , e_{cs}), and phase currents in 0.1A/div(i_{as} , i_{bs} , i_{cs}) where the notations are described in Fig. 3.

In this paper, a new method for detecting the initial grid angle is proposed. In many systems, dc-link voltage is used to supply the auxiliary power for the sensors boards, gating boards, and main control boards. These small loads cause a conduction of the diode before the converter begins to operate and the corresponding phase currents are shown in Fig. 1. From the information of these phase currents, line-to-line source voltage and grid angle are estimated in this paper. To reduce the transient state duration, the Look-Up Table (LUT) which provides an approximated angle according to conduction state of the diodes is used and it reduces the estimator's settling time

conspicuously. Finally, simulation and experimental result are shown in order to verify the feasibility of the proposed scheme.

II. CONVENTIONAL INITIAL ANGLE DETECTION METHOD

In [12], the zero voltage vector is used to obtain the initial angle and the zero vector state remains at least three sampling periods ($3T_s$).

At the zero vector state, the voltage equation of the converter in Fig. 3 can be written as (1) in the d - q stationary reference frame if the interface resistance can be neglected.

$$\begin{aligned} e_{dq}^s &\approx -L_s \frac{di_{dq}^s}{dt} + V_{dq}^s \\ &= -L_s \frac{di_{dq}^s}{dt} + 0 = -L_s \frac{\Delta i_{dq}^s}{\Delta T} \end{aligned} \quad (1)$$

In the equation (1), ΔT is the duration for the current measurement and normally set as $3T_s$. Then, the initial angle can be derived from the phase currents in (2).

$$\theta_e = \arctan \left(-\frac{e_d^s}{e_q^s} \right) = \arctan \left(-\frac{\Delta i_d^s}{\Delta i_q^s} \right) \quad (2)$$

Unfortunately, in this method, considerably large currents may flow if the interface inductance is too small as can be deduced in (1) and it results in the over current trip.

III. PROPOSED INITIAL ANGLE DETECTION METHOD

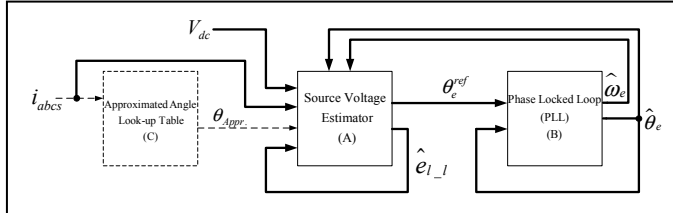


Figure 2. Overall control strategy at the startup of the PWM converter.

The overall control scheme for the initial angle detection of the proposed sensorless PWM converter is depicted in Fig. 2. It consists of source voltage estimator, PLL, and LUT for the approximated angle feed-forward. When the phase currents flow by conducting the diodes, the source voltage estimator operates. From the estimated line-to-line source voltages, the reference of the grid angle can be derived. This angle is used as the input of PLL. When no current flows, all the estimation blocks are bypassed and the grid angle is calculated from the estimated frequency of the source voltage. There are six conduction periods in one cycle of the source voltages. In these conduction periods, the errors of the estimated values are reduced to zero. Thus, the settling time depends on the error between the real grid voltage angle and the initially estimated one. To shorten the settling time, LUT for approximated angle

feed-forward can be used. The details of the estimation scheme are described below.

A. Source Voltage Estimator

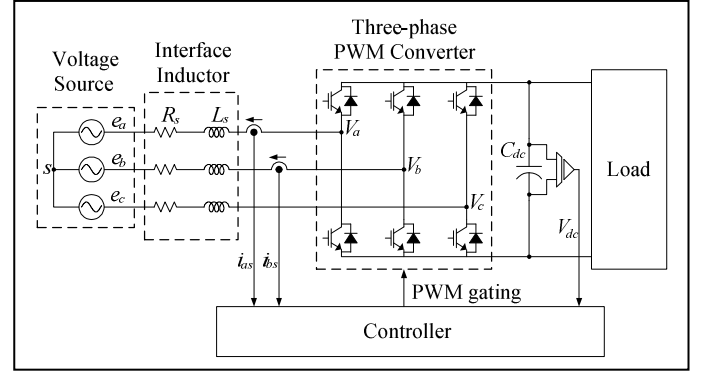


Figure 3. Structure of a source voltage sensorless PWM converter.

The source voltage sensorless PWM converter is depicted in Fig. 3, where e_a , e_b , e_c are the three phase source voltages and V_a , V_b , V_c are the output voltages of the converter. L_s is the inductance and R_s is the resistance of the interface inductor. The dc-link capacitance is C_{dc} . The current sensors measure the phase currents, i_{as} and i_{bs} , and the voltage sensor measures the dc-link voltage, V_{dc} . i_{cs} can be calculated from i_{as} and i_{bs} . The positive direction of phase currents is from the converter to the source as shown in Fig. 3.

The line-to-line voltage equations can be expressed as (3) from the electric circuits.

$$\begin{cases} V_{ab} = R_s(i_{as} - i_{bs}) + L_s \frac{d}{dt}(i_{as} - i_{bs}) + e_{ab} \\ V_{bc} = R_s(i_{bs} - i_{cs}) + L_s \frac{d}{dt}(i_{bs} - i_{cs}) + e_{bc} \\ V_{ca} = R_s(i_{cs} - i_{as}) + L_s \frac{d}{dt}(i_{cs} - i_{as}) + e_{ca} \end{cases} \quad (3)$$

Assuming that i_{as} and i_{bs} flow due to $V_{dc} < e_{ab}$, it is valid that $i_{as} < 0$, $i_{bs} > 0$, $i_{cs} = 0$, $V_{ab} = V_{dc}$, and $i_{as} = -i_{bs}$. In the case that $i_{as} > 0$, V_{ab} is changed to $-V_{dc}$. So, the line-to-line output voltage is determined by the direction of the phase currents. Under this condition, the first equation in (3) can be rewritten as (4).

$$\begin{aligned} -\text{sign}(i_{as}) \times V_{dc} &= R_s(i_{as} - i_{bs}) + L_s \frac{d}{dt}(i_{as} - i_{bs}) + e_{ab} \\ &= 2R_s i_{as} + 2L_s \frac{d}{dt} i_{as} + e_{ab} \end{aligned} \quad (4)$$

From (4), the state equation can be derived as (5), where the states of the estimator are given by $[\hat{i}_{as} \quad \hat{e}_{ab}]^T$.

$$\frac{d}{dt} \begin{bmatrix} \hat{i}_{as} \\ \hat{e}_{ab} \end{bmatrix} = \begin{bmatrix} -\frac{R_s}{L_s} & -\frac{1}{2L_s} \\ 0 & 0 \end{bmatrix} \begin{bmatrix} \hat{i}_{as} \\ \hat{e}_{ab} \end{bmatrix} - sign(i_{as}) \begin{bmatrix} \frac{1}{2L_s} \\ 0 \end{bmatrix} V_{dc} + G(i_{as} - \hat{i}_{as}) \quad (5)$$

The superscript “ $\hat{\cdot}$ ” indicates the estimated state. If the gain of the estimator is set as (6), its characteristic equation has double roots. ω_o denotes the pole of the characteristic equation.

$$G = \begin{bmatrix} g_1 \\ g_2 \end{bmatrix} = \begin{bmatrix} 2\omega_o - \frac{R_s}{L_s} \\ -2L_s\omega_o^2 \end{bmatrix} \quad (6)$$

For three phase balanced system, three estimators are needed. Namely, if a- and b-phase currents flow, one of three estimators gives the estimated line-to-line source value, \hat{e}_{ab} . Assuming that three phase source voltages are given by (7) in the stationary reference frame, the relationships between line-to-line source voltages can be expressed by (8). From (8) and \hat{e}_{ab} , the other two voltages (\hat{e}_{bc} , \hat{e}_{ca}) are derived simply.

$$\begin{cases} e_a = -E_m \sin \theta_e \\ e_b = -E_m \sin(\theta_e - 2\pi/3) \\ e_c = -E_m \sin(\theta_e + 2\pi/3) \end{cases} \quad (7)$$

where E_m is the peak value of the line-to-neutral source voltage.

$$\begin{cases} \frac{e_{ab}}{e_{bc}} = \frac{1+\sqrt{3} \tan \theta_e}{-2} \\ \frac{e_{bc}}{e_{ca}} = \frac{-2}{1-\sqrt{3} \tan \theta_e} \\ \frac{e_{ca}}{e_{ab}} = \frac{1-\sqrt{3} \tan \theta_e}{1+\sqrt{3} \tan \theta_e} \end{cases} \quad (8)$$

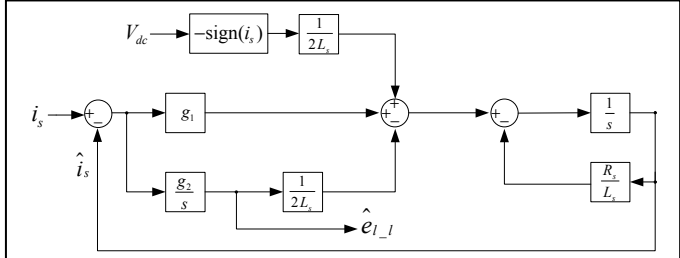


Figure 4. Line-to-line source voltage estimator in stationary reference frame.

Fig.4 shows the source voltage estimator. Phase current and estimated line-to-line source voltage are expressed by i_s and \hat{e}_{l_l} , respectively.

The estimated line-to-line source voltage can be rewritten as (9) in the $d-q$ stationary reference frame.

$$\begin{cases} \hat{e}_{ds}^s = \frac{1}{3}(2\hat{e}_{as} - \hat{e}_{bs} - \hat{e}_{cs}) = \frac{1}{3}(\hat{e}_{ab} - \hat{e}_{ca}) = -E_m \sin \theta_e^{ref} \\ \hat{e}_{qs}^s = \frac{1}{\sqrt{3}}(\hat{e}_{bs} - \hat{e}_{cs}) = \frac{1}{\sqrt{3}}\hat{e}_{bc} = E_m \cos \theta_e^{ref} \end{cases} \quad (9)$$

where \hat{e}_{ds}^s and \hat{e}_{qs}^s are estimated d- and q-axis source voltages, respectively.

The reference angle (θ_e^{ref}) used as an input of the PLL can be derived as (10).

$$\theta_e^{ref} = \arctan \left(\frac{-\hat{e}_{ds}^s}{\hat{e}_{qs}^s} \right) \quad (10)$$

In the bypassed period, meanwhile, the estimators in Fig. 4 are turned off and the estimated grid angle, $\hat{\theta}_e$ can be calculated from (11) using the estimated angular frequency of the source voltage, $\hat{\omega}_e$.

$$\hat{\theta}_e = \int \hat{\omega}_e dt + \hat{\theta}_{eo} \quad (11)$$

where $\hat{\theta}_{eo}$ is the initial value of the integrator at the instant where the bypass period starts.

B. Phase Locked Loop (PLL)

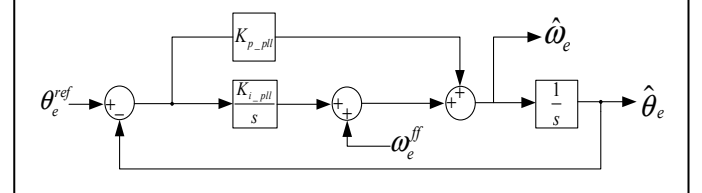


Figure 5. Grid angle estimator using PLL.

The grid angle estimator is shown in Fig.5. This PLL operates simultaneously with the source voltage estimator. The closed-loop transfer function between the reference source voltage angle and the estimated one is derived as (12).

$$\frac{\hat{\theta}_e}{\theta_e^{ref}} = \frac{K_{p_pll}s + K_{i_pll}}{s^2 + K_{p_pll}s + K_{i_pll}} \quad (12)$$

where K_{p_pll} and K_{i_pll} denotes the proportional and integral (PI) gains, respectively. If the PI gains are set as $K_{p_pll} = \zeta \omega_{c_pll}$ and $K_{i_pll} = \omega_{c_pll}^2$ respectively, (12) works as a second order low-pass filter which has a zero. Here, ω_{c_pll} and ζ represent a cut-off frequency and damping coefficient of the PLL, respectively.

$$\frac{\hat{\theta}_e}{\theta_e^{ref}} = \frac{\zeta \omega_{c_pll}s + \omega_{c_pll}^2}{s^2 + \zeta \omega_{c_pll}s + \omega_{c_pll}^2} \quad (13)$$

C. Look Up Table (LUT) of Approximated Angle

TABLE I. APPROXIMATED ANGLE ACCORDING TO DIRECTIONS OF PHASE CURRENTS

Direction of Phase Current			Approximated Initial Angle[rad.]
i_{as}	i_{bs}	i_{cs}	
(0)	(+)	(-)	$-\pi$
(-)	(+)	(0)	$-2\pi/3$
(-)	(0)	(+)	$-\pi/3$
(0)	(-)	(+)	0
(+)	(-)	(0)	$\pi/3$
(+)	(0)	(-)	$2\pi/3$
(0)	(0)	(0)	unknown

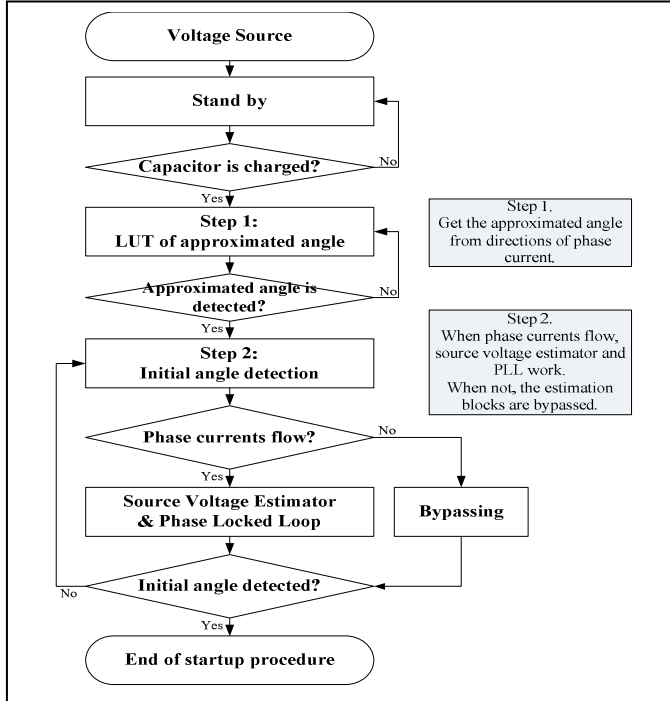


Figure 6. Flow chart of proposed operating sequence for initial angle detection.

If the estimated grid angle starts from zero, the initial transient time of the estimation will be highly affected by the initial grid angle. Because the diode conduction always occurs near the peak of the line-to-line voltage, the grid angle can be approximated according to the diode conduction state as shown in Table I. That is, the approximated grid angle can be uniquely extracted from the direction of the phase currents. For example, if b-phase current is positive and c-phase current is negative, the grid angle is near $-\pi$ [rad.]. Using this LUT, the initial error of the grid angle can be reduced as small as the approximation error and the initial transient time reduces conspicuously. Finally, the proposed operating sequence is depicted as a flow chart in Fig.6.

IV. SIMULATION RESULTS

TABLE II. SIMULATION PARAMETERS

Parameter	Value
Line-to-line source voltage	220[V _{rms}]
Frequency	60[Hz]
Interface inductance	0.1[mH]/1.5[mH]/5[mH]
Interface resistance	0.1[Ω]
Dc-link capacitance	3300[μF]
Light load	10[kΩ]

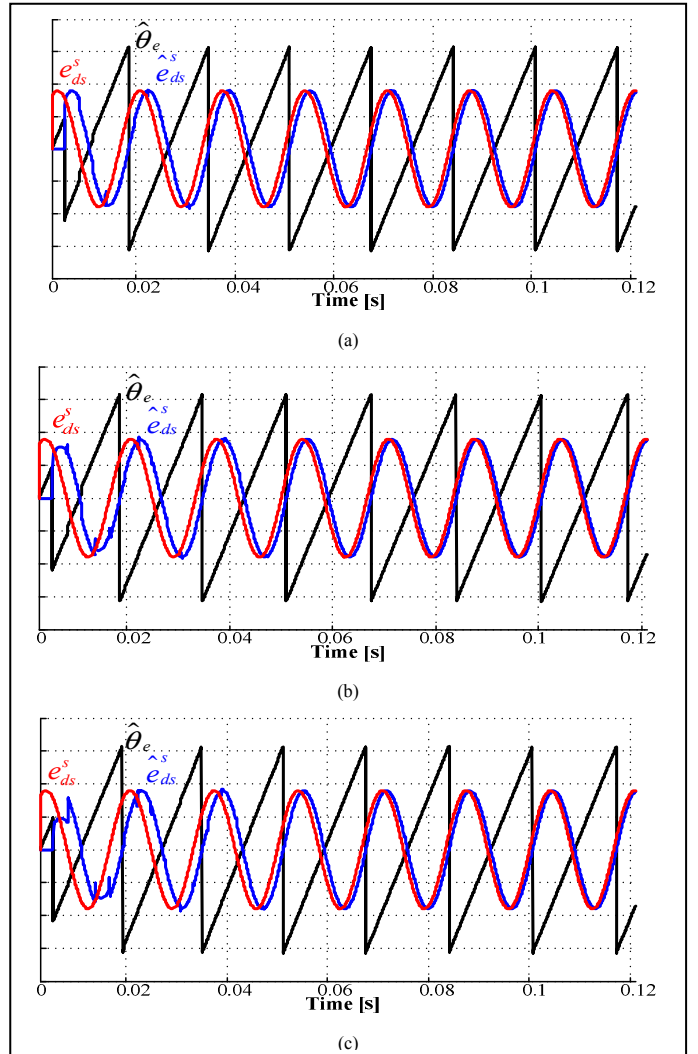


Figure 7. Simulation results (e_{ds}^s , \hat{e}_s^s : 100 V/div, $\hat{\theta}_e$: 1 rad/div) : (a): $L_s = 0.1[mH]$, (b): $L_s = 1.5[mH]$, (c): $L_s = 5[mH]$

To verify the feasibility of the proposed initial angle detection method, computer simulation has been performed by MATLAB Simulink. The system parameters used in the simulation are listed in Table II. The simulation is performed in three cases that the interface inductances are $0.1[mH]$, $1.5[mH]$, and $5[mH]$, respectively. The sequence of the estimation by the approximated angle from LUT was excluded

at these cases. As shown in Fig. 7, it takes less than 0.1[s] that the estimations settles down for all cases. Even though there is a large difference in the inductance values, the time is almost the same. Therefore, this simulation result shows the settling time is not largely related with the inductance of the interface inductor.

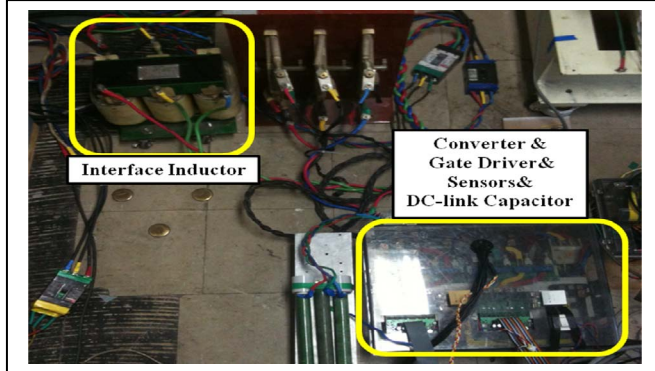


Figure 8. Experimental setup

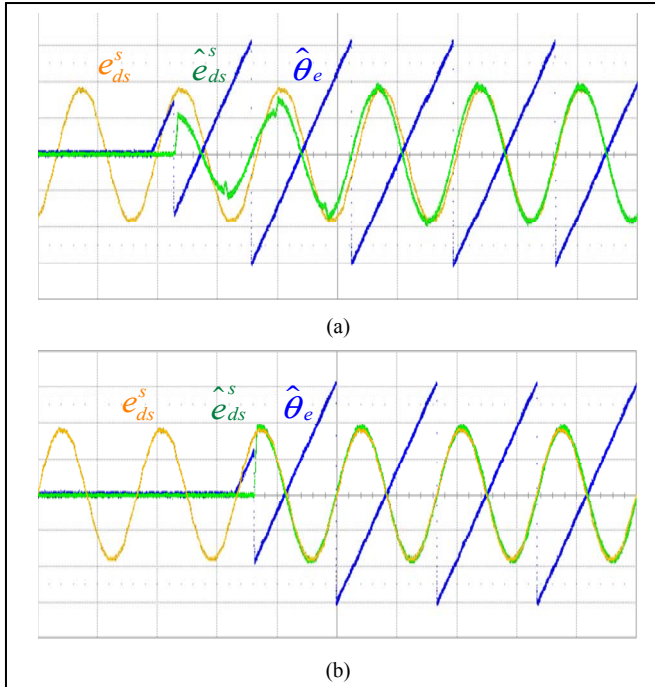


Figure 9. Experimental results (e_{ds}^s , \hat{e}_{ds}^s : 100 V/div, $\hat{\theta}_e$: 1 rad/div, Time: 10ms/div). (a) without LUT. (b) with LUT.

V. EXPERIMENTAL RESULTS

To evaluate the validity of the proposed initial angle detection method, an experiment has been performed. The experimental setup is shown in Fig. 8. The PWM converter has been connected to the three phase grid of which line-to-line voltage is $220[V_{rms}]/60[Hz]$. The interface inductance is $1.5[mH]$ and the dc-link capacitance is $3300[\mu F]$.

Fig. 9(a) and (b) show the initial angle estimation results according to the use of the approximated angle LUT. When the

LUT is not applied, the initial estimation takes about three or four cycles of the source voltage as shown in Fig. 9(a). On the other hand, it takes only a half cycle of the source voltage when the LUT is applied. It can be shown that the LUT improves the initial estimation performance.

VI. CONCLUSIONS

This paper proposed a method of the initial angle detection for smooth starting of PWM converter. The estimation strategy to avoid the deterioration in the performance at the startup of the control has been described. Using the proposed method, the accurate grid angle can be estimated within a half cycle of the source voltage regardless of the size of the interface inductor. The simulation has verified that small interface inductance can be used due to this method. And in experimental result, proposed LUT makes the initial transient time reduced.

REFERENCES

- [1] N.R. Zargari and G. Joos, "Performance investigation of a current controlled voltage regulated PWM rectifier in rotating and stationary frames," IEEE Trans. Ind. Electron., vol. 42, no. 4, pp.396-401, Aug. 1995.
- [2] V.Blasco and V.Kaura, "A new mathematical model and control of a three-phase AC-DC voltage source converter," IEEE Trans. Power Electron., vol. 12, no. 1, pp.116-123, Jan. 1997.
- [3] J.W. Choi and S.K. Sul, "Fast current controller in three-phase ac/dc boost converter using d-q axis crosscoupling," IEEE Trans. Power Electron., vol. 13, no.1, pp.179-185, Jan. 1998.
- [4] R.Wu, S.B. Dewan, and G.R.Slemon, "Analysis of an ac-to-dc voltage source converter using PWM with fixed switching frequency," IEEE Trans. Ind. Appl., vol.27, no.2, pp.355-364, Mar./Apr. 1991.
- [5] T.Ohnishi and K. Fujii, "Line voltage sensorless three phase PWM converter by tracking control of operating frequency, Proceedings of Power Conversion Conference, 1997, pp.247-252.
- [6] T. Noguchi, H.Tomiki, S. Kondo, and I. Takahashi, "Direct Power Control of PWM Converter Without Power-Source Voltage Sensors, IEEE Transactions on Industry Applications, vol.34, no.3, pp.473-479, 1998.
- [7] S. Hansen, M. Malinowski, F. Blaabjerg, and M.P. Kazmierkowski, "Sensorless control strategy for PWM rectifier," 15th Annual IEEE Applied Power Electronics Conference and Exposition, 2000, pp.832-838.
- [8] E. Jung, M. Kim and S.K.Sul, "Control Scheme for Source Voltage Sensorless PWM Converters under Source Voltage Unbalance," Power Electronics and Application, 14th European Conference, 2011, pp.1-pp.10.
- [9] H.S.Song, I.W.Joo, and K.Nam, "Source Voltage Sensorless Estimation Scheme for PWM Rectifiers Under Unbalanced conditions, IEEE Transactions on Industrial Electronics, vol. 50, no.6, pp.1238-1245, 2003.
- [10] B.H.Kwon, J.H. Youm, and J.W. Lim, "A line-voltage-sensorless synchronous rectifier," IEEE Trans. Power Electron., vol.14, no.5, pp.966-972, Sep. 1999.
- [11] I.Agirman and V.Blasko, "A novel control method of a VSC without AC line voltage sensors," IEEE Trans. Ind. Appl., vol. 39, no.2, pp.519-524, Mar./Apr. 2003.
- [12] H. Yoo, J.H. Kim, and S.K.Sul, "Sensorless Operation of a PWM Rectifier for a Distributed Generation, IEEE Transactions on Power Electronics, vol.22, no.3, pp.1014-1018, 2007.